Concepts for Processing and Analyzing of Multiple SAR and Landsat Images

J. Thomas, R. Mullen, F. Leberl, W. Kober
VEXCEL Corp.
Boulder CO.

J. Cimino
Jet Propulsion Laboratory
Pasadena CA.

ABSTRACT

The use and application of multi-sensor data sets are an absolute necessity for remote sensing to fulfill its promise. Initial efforts of registering dissimilar images have been made, but results are not widely available. This paper describes some initial work to better understand the difficulties of multi-sensor registration. Accuracies achieved are in excess of a pixel diameter.

Key Words: Multi-sensor, registration, SAR, Landsat, SIR-B, registration accuracy.

1. Introduction

The present paper reports on some preliminary results of an empirical study to examine the problems of interactive registration of differing selected imagery types. This problem domain is complex due to dissimilar ties in images that need to be matched, i.e. registered or fused.

Another purpose is to understand and interpret corresponding image intensity variations. In particular, those variations to be examined are functions of:

- wavelength;
- incidence angle;
- polarization;
- time of image acquisition;
  - illumination changes
  - scene content changes
- type of sensor

An eventual goal will be a capability for the creation of data products from multi-sensor, multi-temporal sources, which delineate regions corresponding to intensity variations as a function of selected variables.

Dissimilar image matching has an extensive literature. An early contribution by [Mader, 76] addressed SAR and Landsat-3-RBV. Many similar efforts followed, essentially relying on manual techniques. A recent review by Leberl (1986) enumerated 90 references. Automating the task reliably remains elusive. Even matching ascending and descending orbit SAR images can pose great difficulties because of local intensity reversals. In [McConnell, 87] the binarized regions derived from Marr-Hildreth edges are employed to match orbit in variant SAR image contents. Edges and invariant moments were used in [Wong, 79] for SAR-optical imagery matching.

The following will describe a more elaborate dataset then is commonly used, but it is still short of what is expected in the EOS-era [EOS, 88]. The following discussion describes some of the difficulties involved in achieving sub-pixel registration accuracy.

2. Description of Experimental Datasets

The following experimental dataset was used to develop experience in multi-sensor processing.

The sensor source and quantities of each image type were:

- Landsat TM (7 bands);
- SIR-B SAR (1 image);
- Aircraft SAR (2 overflights)

Relevant available parameters for each type are described in Table 1.

The imaged scene was Raisin City, CA. The topography is flat, and the major man-made features are Raisin City itself and Henderson Road. The foliage types consist of orchards and various crops. The orchards contain walnuts, beach, plum and almond. The crops were alfalfa, corn, beans, tomatoes, and cotton. The relevant crop descriptors are:

- % ground cover by crop type;
- crop state;
- time period;
- location

3. Registration Methodology

Our experimental work is designed to provide experience that will lead to the development of automated routines for multi-sensor image registration.

Achieving the highest fidelity co-registration of all imagery sets to a map, ie. geocoding, is expected to require first registering the highest resolution imagery, in this case the aircraft SAR, to map coordinates. The subsequent registration of lower resolution imagery to this higher resolution data set can be accomplished either by up-sampling the former or down-sampling the latter.

If centralized terrain topography were involved in the imaged scene, then added procedural complexity would be present. For SAR images, geocoding methods for real satellite imagery [Kwok, 87], [Curlander, 82,84,87] could be used with modification for real aircraft SAR images. Such modifications would be required to take into account the differing phase compensations for the aircraft scenario from the satellite case. But because the imaged scene is topographically flat, such terrain compensations were not required in this case.

However, another problem arises with SAR because the aircraft slant plane SAR data

is complex quadpole polarization imagery. This allows any desired combination of transmit and received polarizations to be incorporated into any real slant plane SAR image. Therefore, the most efficient method would be to first geocode the complex data. Then any real SAR image with desired polarization combinations subsequently created from this geocoded complex data would automatically be geocoded.

However, geocoding complex data requires interpolating phase as well as amplitude data. Efficient methods for interpolating the more sensitive phase data are the subject of ongoing research. No results are presented using complex interpolation.

Therefore, each real slant plane aircraft SAR image, for a particular polarization combination, was first created and then separately geocoded. The first aircraft SAR image was registered to a 1:24,000 map of Raisin City to yield the base image. The control points that were used were road intersections and other well defined points in both the image and map.

Examples of the SIR-B SAR, aircraft SAR, and Landsat images are shown in Fig. 1-3 respectively. The mapping of the control points leads to a so-called deformation grid, shown in Fig. 4. This grid is then used to generate the final resampling of pixels for a geocoded image. The resampled aircraft SAR image is shown in Fig. 5. The effects of range curvature are clearly evident.

The actual registration quality depends on an ability to use context in the matching process. Automated techniques incorporate such context by matching areas and edges. Manual techniques need an ability to interactively shift the two datasets over one another.

The other images were also registered to the map using similar control points. There were some clearly visible

misregistrations relative to the base image, as shown in Fig. 6-7.

To reduce these registration errors, the remaining images were re-warped again to fit the base image by the use of corresponding control points in the images. These results are shown in Fig. 8-9.

The number of control points used, their spatial distribution, and the resulting deformation grids were plotted in each case. Using the deformation grid, the errors at each of the control points were calculated, as shown in Fig. 4. A summary of the registration error statistics is tabulated in Table 2.

4. Preliminary Discussion of Results

It is to be noted that the overall accuracies of multi-sensor registration varies in excess of one pixel for all image-to-map registrations. Image-to-image registration also tended to have residual errors of several pixels at the higher resolution, but one pixel or less at the lower resolution.

The slant range format of the aircraft SAR images involves considerable distortion from a ground plane geocoded image. In addition, the noise and speckle present in both the aircraft and SIR-B imagery made the identification of control points difficult.

The identification of common control points in the dissimilar image sets with the corresponding control points in the base image was also difficult because of intensity variations arising from differences in wavelength. The problem of relating TM data to radar was especially severe.
This is not surprising given earlier reports about similar efforts [Leberl, 86].

The problem of recognizing common regions with intensity differences dependent on wavelength effects is not tractably

wavelength effects is not tractably resolved using local histogram remapping. In general, this problem is overcome using common perceived edges. However, this process is difficult to automate because there are edges which are not common to all imagery types and edges tend to break up differently even among the radar images.

5. Conclusions

Interpretation of intensity differences in multi-sensor images is an ongoing activity. A need exists to develop automated techniques for matching of dissimilar images. Subsequent to that, a qualitative understanding needs to be developed relating image intensities to physical properties of imaged objects, such as crop descriptors, and to sensor parameters.

Considerable effort has been expanded in past studies of multi-sensor datasets. Unfortunately, the sheer difficulty of the initial data registration task usually resulted in a scenario where most of a project's time and resources were spent on registration. Consequently, the actual study of registered image contents and their parametric variations tended to suffer.

It is clear that improved technology for registration must be developed to reduce the drudgery and wasted effort of mundane data preparation from the scientific analysis of multi-sensor datasets.

We have begun to study avenues for automating the multi-sensor registration process and report on first qualitative results. We conclude that sub-pixel accuracies will be a difficult goal to reach.

References

1. Kwok, R. et al., "Rectification of Terrain Induced Distortions in Radar Imagery," Photog. Eng. Rem. Sens., vol. 53, #5, May 1967.

2. Curlander, J., "Location of Spaceborne SAR Imagery," IEEE Trans. Geo. Rem. Sens., GE-20, #3, July 1982.

3. Curlander J., "Utilization of Spaceborne SAR Data for Mapping," IEEE Trans. Geo. Rem. Sens., GE-22, #2, Mar. 1984.

4. Curlander J. et al., "A post-processing system for automated rectification and registration of spaceborne SAR imagery," Int. J. Rem. Sens., vol-8, #4, 1987.

5. Mader, G., McCaudless W., "Space Based Topographic Mapping Experiment Using Seasat-SAR and Landsat-3-RBV Imagery", Phoenix Corp., McLean, VA 22102, 1981.

6. Leberl, F., "Review of Basic Techniques for Multi-Sensor and Image Time Series Analysis", VEXCEL Technical Report #100986 (to European Space Agency), Boulder, CO 80201, Oct. 1986.

7. McConnell, R., "Matching of Dissimilar Radar Images Using Marr-Hildreth Zero Crossings", Proc. Amer. Soc. Photog. Rem. Sens., Balt., MD, April 1987.

8. From Pattern to Process: The Strategy of the Earth Observing System, EOS Science Steering Committee Report Vol. II NASA, 1988.

9. Wong, R., "Radar to Optical Scene Matching", Proc. SPIE, Vol. 186, 1979.

A) Aircraft SAR
- Resolution = 7.495 m in range; 10.98 m in azimuth
- Image size = 1024 x 1024 pixels
- Wavelength = L-Band
- Polarization = complex quadpole
- Flying height = 12221 m
- Incidence angle
- Time of acquisition
  - 9/28/84 21:04:55
  - 9/28/84 20:50:38

B) SIR-B SAR
- Resolution = 34.6 m ground range; 28.5 m azimuth; 12.5 m pixel size
- Image size = 7000 x 2957
- Wavelength = L-Band (23 cm)
- Polarization = HH
- Flying height = 235 km
- Incidence angle = 24.0 deg.
- Time of acquisition
  - 284/ 12:17:26.744 (1984)
- Ascending orbit

C) Landsat TM
- Resolution = 30 m Bands 1-6; 120 m Band 7
- Image size = 4320 x 2984
- Wavelength
  - Band 1 = .45 - .52 um
  - Band 2 = .52 - .60 um
  - Band 3 = .63 - .69 um
  - Band 4 = .76 - .90 um
  - Band 5 = 1.55 - 1.75 um
  - Band 6 = 10.40 - 12.50 um
  - Band 7 = 2.08 -2.35 um
- Flying height = 705 km
- Time of acquisition = not available

Parameters Of The Multi-Sensor Dataset

Table 1

Image Types Matched	RMS Pixel Errors X	RMS Pixel Errors Y	Pixel Size	RMS Metric Errors X	RMS Metric Errors Y	Total # Pixels	# Controls
(1) Aircraft #1 to Map	2.83	1.40	10.0m	28.3m	14.0m	1200 x 1100	25
(2) SIR-B to Map	1.86	1.95	12.5m	23.3m	24.4m	1200 x 1200	30
(3) (2) to (1)	2.39	1.29	10.0m	23.9m	12.9m	1100 x 1000	37
(4) TM to Map	0.40	0.39	30.0m	12.0m	11.7m	1300 x 1300	30
(5) (4) to (1)	2.35	1.55	10.0m	23.5m	15.5m	1100 x 1100	38
(6) Aircraft #2 to Map	1.79	1.30	10.0m	17.9m	13.0m	1200 x 1100	21
(7) (6) to (1)	2.40	2.27	10.0m	24.0m	22.7m	1100 x 1000	54

Summary Statistics of Registration Errors

Table 2

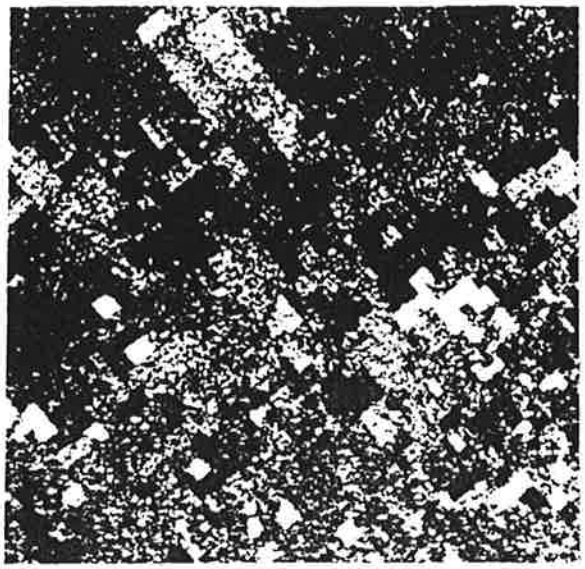

Original SIR-B SAR Image

Figure 1

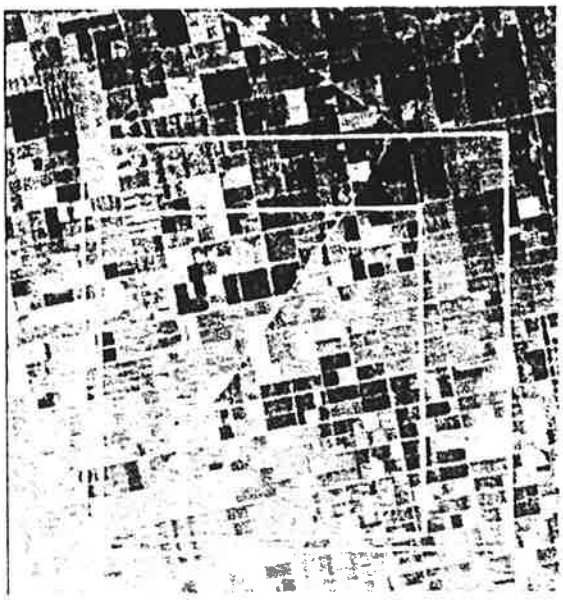

Original Landsat TM Image
Outer Box Registered to Map
Inner Box Registered to Map Registered Aircraft SAR

Figure 3

Original Aircraft SAR Image

Figure 2

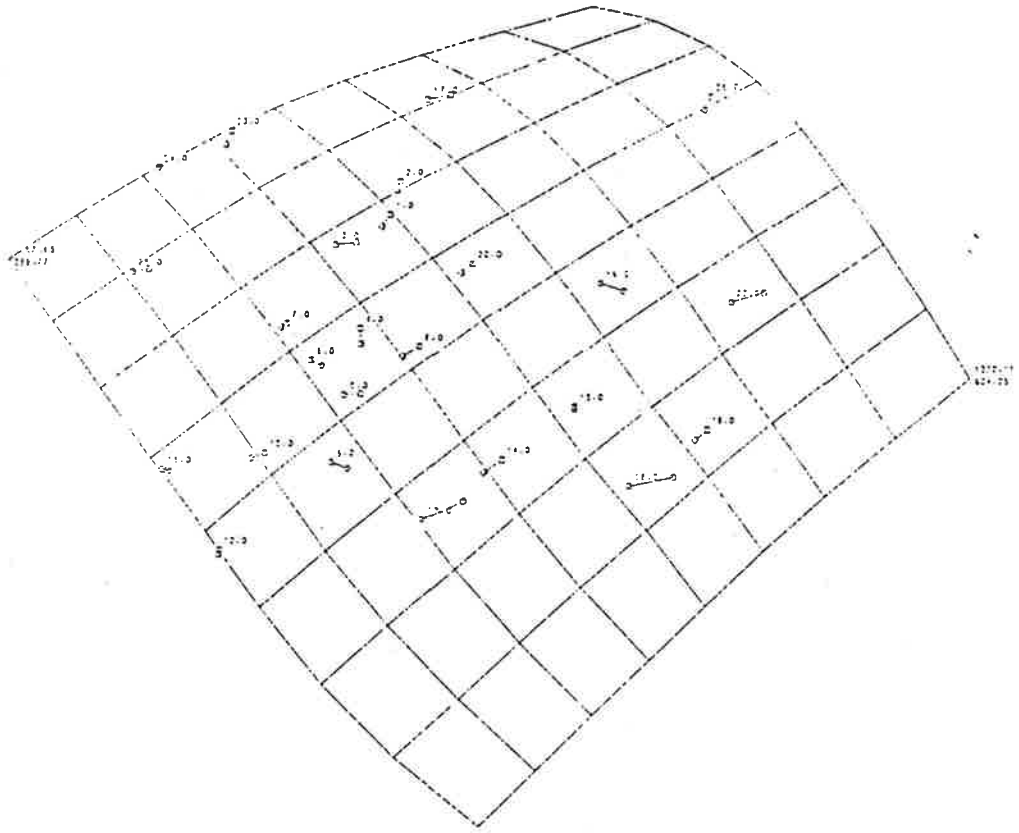

Registration Deformation Grid
for Aircraft SAR Image

Figure 4

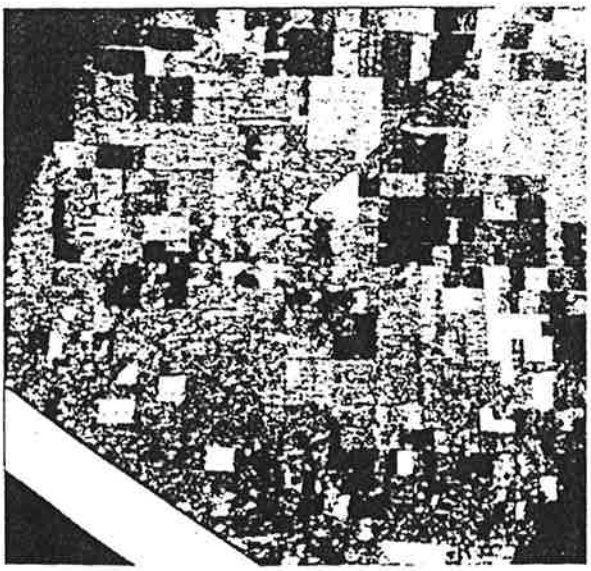

Aircraft SAR Image Registered to Map

Figure 5

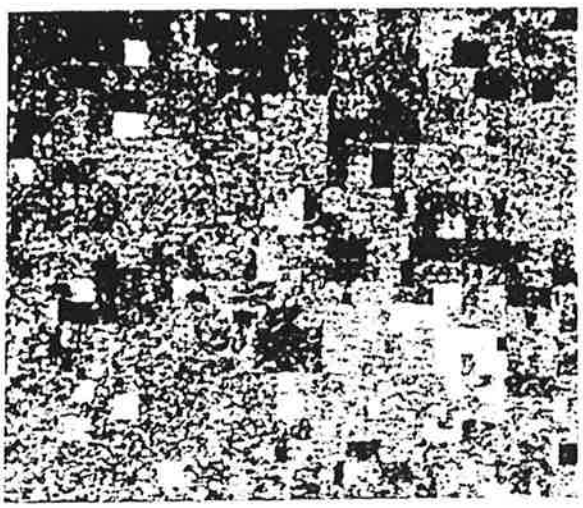

SIR-B Image Registered to Map

Figure 6

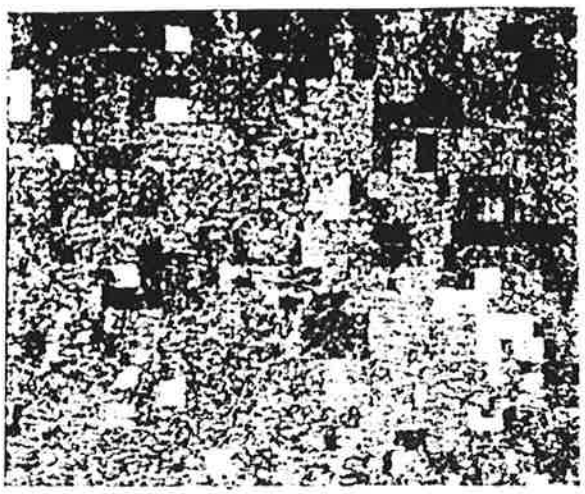

SIR-B Image Registered to Geocoded Aircraft SAR Image

Figure 8

Landsat TM Image Registered to Map
TM Image Registered to Map
Box Corresponds to Inner Box of Fig. 3

Figure 7

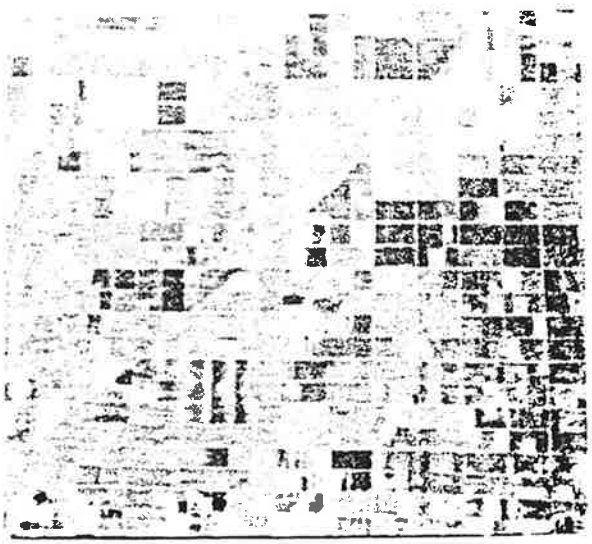

Landsat TM Image Registered to Geocoded Aircraft SAR Image

Figure 9